

Mineralogical Transformations in Altasteel Electric Arc Furnace Dust Roasted with Na₂CO₃ and Secondary Ferrite-Forming Additives

P. C. Holloway and T. H. Etsell

*Department of Chemical and Materials Engineering,
University of Alberta, Edmonton, Alberta, Canada T6G 2G6
Email: prestonh@ualberta.net*

ABSTRACT

The effect of secondary additives, such as CaCO₃ and MnCO₃, on the mineralogical transformations in Altasteel EAF dust (9.4% Zn, 31.9% Fe) during roasting with Na₂CO₃, and metal extractions during hot water and H₂SO₄ leaching of the roasted residues, was studied using a combination of techniques, including Design of Experiments testing, x-ray diffraction, scanning electron microscope/energy dispersive x-ray analysis and chemical analysis. The research objective was to promote the formation of acid insoluble metal ferrites during roasting to try to lower iron extractions during acid leaching.

Neither additive was effective in reducing iron extractions due to the unexpected mineralogical changes caused during roasting by the addition of these secondary additives to this poorly crystalline EAF dust. Low CaCO₃ or MnCO₃ additions promoted the formation of manganese rich iron oxides (e.g., Mn₂FeO₄), instead of MnFe₂O₄, which caused more iron to be available to react with Na₂CO₃ during roasting to form acid soluble NaFeO₂. Increased CaCO₃ additions further increased iron extractions, by further increasing the formation of Mn₂FeO₄ ferrites, but increased MnCO₃ additions at roasting temperatures above 950°C led to the formation of a ZnFe₂O₄-MnFe₂O₄ solid solution. While this resulted in lower iron extractions, lower overall zinc recoveries during acid leaching were also observed.

Keywords: *Electric arc furnace dust, Phase transformations, Pyrometallurgy, Leaching, Sodium carbonate roasting*

1. INTRODUCTION

Electric arc furnace (EAF) dust is produced globally as a byproduct of EAF steelmaking as a result of the interactions of metallic iron, volatilized metal oxides, and other slag components in the gas phase above the electric arc furnaces [1]. The resulting dust is predominantly a magnetite-franklinite-jacobsite (Fe₃O₄/ZnFe₂O₄/MnFe₂O₄) solid

solution, but also contains significant quantities of toxic elements or deleterious impurities, such as Pb, Cd, Cr, Cl and F, which not only make the dust difficult to treat, but also cause it to fail toxicity leaching requirements, resulting in the classification of EAF dust as a hazardous waste [2]. Treatment or disposal of the EAF dust is an expensive and global problem, with about 1.8 million tonnes per year produced in North America, Europe and Japan [3,4] and treatment or disposal costs as high as \$2 to 3 US per tonne of steel produced [4].

In spite of significant research globally into the treatment of EAF dust, Waelz kiln processing remains the dominant treatment technology with 80 to 85% of the EAF dust in the US [5] and up to 76% worldwide [6] treated in Waelz kilns, in spite of the high energy consumption, the production of relatively low quality zinc products and the general inability to recycle the iron values from the dust back to the steel furnaces. Economics and product purity from Waelz kiln processing dictate the non-localized treatment of the dust near electrothermic or Imperial Smelting Process zinc smelters or chemical or fertilizer plants that can accept the zinc product.

Transformational roasting, or roasting where a solid reagent is added which reacts with the feed material in the solid state to produce a desirable mineralogical change in the starting material, to treat EAF dusts has been proposed as a potential alternative to Waelz kiln processing [7]. Transformational roasting would, ideally, use pyro- and hydrometallurgical operations synergistically to achieve high metal recoveries while lowering the volume and increasing the disposability of the residues produced.

Initial tests into transformational roasting of a sample of EAF dust from the Scaw Metals' Altasteel plant in Edmonton, Alberta, Canada, indicated that roasting with 45% Na_2CO_3 at 1000°C results in zinc extractions of up to 94% after leaching with 200 g/L H_2SO_4 , with 55% of the iron also dissolved [7]. (Leaching the same roasted material with NaOH resulted in zinc extractions of 43%, lead extractions of 13%, and negligible iron extractions [7].) Mineralogically, the mixture of zinc-iron-manganese ((Zn,Mn,Fe)(Fe,Mn) $_2\text{O}_4$) spinels in the EAF dust reacts with Na_2CO_3 to form α - and β - NaFeO_2 and CaCO_3 reacts with Fe_3O_4 in the dust to form srebrodolskite ($\text{Ca}_2\text{Fe}_2\text{O}_5$) during roasting [7]. Leaching the roasted EAF dust with hot water dissolves any unreacted Na_2CO_3 , or Na_2O or Na_2SO_4 formed during roasting, and any Na-Cr, Na-Mo, or Na-V compounds formed during roasting while ZnO, NaFeO_2 , $\text{Ca}_2\text{Fe}_2\text{O}_5$ and Ca_2SiO_4 are dissolved during subsequent acid leaching to produce a residue consisting of gypsum ($\text{CaSO}_4 \cdot 2\text{H}_2\text{O}$), magnetite (Fe_3O_4) and jacobsite (MnFe_2O_4) [7].

Research on Na_2CO_3 roasting of another ferrite-containing waste (i.e., zinc ferrite residue from La Oroya, Peru) indicated that the addition of secondary additives, such as CaCO_3 or MnCO_3 , could be used to decrease iron extractions in H_2SO_4 leaching through the formation of acid insoluble metal ferrites during roasting [8]. Mineralogical studies from the roasting of the Altasteel EAF dust with Na_2CO_3 show that a significant proportion of the iron forms minerals that are insoluble in 200 g/L H_2SO_4 solutions [7], but further reductions in iron extraction, if high zinc and chromium recoveries could be maintained, would be advantageous in processing the EAF dust with Na_2CO_3 roasting.

This paper discusses the effects of secondary additives, such as CaCO_3 and MnCO_3 , on the mineralogical transformations in the Altasteel EAF dust during roasting with Na_2CO_3 , and metal extractions during leaching of the roasted residues. A combination of techniques were used, including Design of Experiments testing, x-ray diffraction (XRD), scanning electron microscope (SEM)/energy dispersive x-ray (EDX) analysis and chemical analysis, to ascertain the minerals formed, and their relative proportions, with particular focus on changes in the type and quantity of iron minerals formed during roasting.

2. FEED MATERIALS

Electric arc furnace dust is produced as a byproduct of the recycling and production of carbon steel at Altasteel's plant at a rate of 15000 t/y [9]. A chemical analysis of the sample obtained from Altasteel is presented in Table 1. Elements, such as Cr, F and Pb, are of particular concern, as it is usually based on these elements that the dust fails Toxicity Characteristic Leaching Procedure (TCLP) tests and is then classified as a hazardous waste [9].

Table 1 Chemical Analysis of As-Received Altasteel EAF Dust

Analysis, %						Analysis, ppm	
Al	0.50	Cr	0.34	K	0.82	Co	70
As	0.04	Cu	0.40	Si	1.92	F	130
Cd	0.03	Fe	31.9	Na	1.32	Mo	150
Ca	7.14	Pb	0.90	S	0.43	Ni	390
C	4.71	Mg	1.39	Zn	9.40	V	80
Cl	1.45	Mn	3.56				

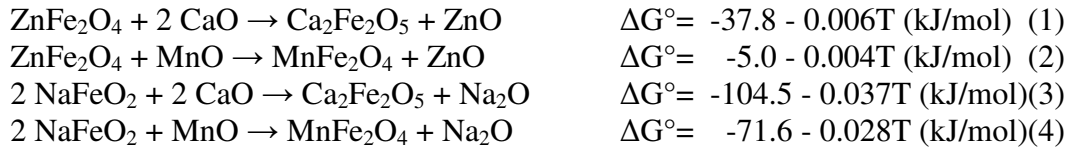
The as-received EAF dust had a particle size of 50% passing 84 μm , but with almost 35% greater than 417 μm . After drying the residue, the oversize was pulverized to give a final particle size of 90% passing 75 μm for the EAF dust used in the roasting tests.

Mineralogically, x-ray diffraction analysis shows that the Altasteel EAF dust contains a mixture of Zn-Mn-Fe spinels ($(\text{Zn,Mn,Fe})(\text{Fe,Mn})_2\text{O}_4$), CaCO_3 , NaCl , $\text{CaZn}_2(\text{OH})_6 \cdot 2\text{H}_2\text{O}$ and larnite (Ca_2SiO_4), but several different analyses, including x-ray diffraction, scanning electron microscopy (SEM) imaging, energy dispersive x-ray analysis (EDX) and diagnostic leaching, strongly indicated that the EAF dust is much less crystalline than zinc ferrite materials produced from zinc sulphide roasting [7].

3. BACKGROUND

Thermodynamically, calcium and manganese ferrites should be more thermodynamically favorable ferrites than franklinite (ZnFe_2O_4) or NaFeO_2 and recent studies indicate that both srebrodolskite ($\text{Ca}_2\text{Fe}_2\text{O}_5$) and manganese ferrites, such as

jacobsite (MnFe_2O_4), can be formed during roasting of zinc ferrite materials with Na_2CO_3 along with secondary additives, such as CaCO_3 and MnCO_3 [8].



All thermodynamic data reported in this article was obtained from either the FREED or FACTSAGE thermodynamic databases. FREED is a trademark of THERMART. FACTSAGE is a trademark of Thermafact/CRCT and GTT-Technologies.

Mineralogical results from the roasting of Altasteel EAF dust with Na_2CO_3 indicate that both $\text{Ca}_2\text{Fe}_2\text{O}_5$ and MnFe_2O_4 are present, along with Fe_3O_4 and NaFeO_2 , after roasting and MnFe_2O_4 , in particular, plays a role in reducing the overall iron extraction during acid leaching observed from these roasted samples [7]. While these results are favorable, further reductions in iron extractions would be advantageous and, thus, design of experiments (DOE) testing were performed to determine whether secondary additions of CaCO_3 or MnCO_3 during Na_2CO_3 roasting could further promote the formation of acid insoluble metal ferrites and further depress iron extractions during H_2SO_4 leaching while maintaining high zinc and chromium extractions.

4. PROCEDURE

4.1. Roasting and Leaching Tests

Dried Altasteel EAF dust was mixed with a certain weight of Na_2CO_3 in a mortar and pestle and this mixture was transferred to an alumina crucible, heated to the reaction temperature and roasted in a muffle furnace in air for 5 h. The samples were removed from the furnace, air cooled, and ground to a uniform particle size and a subsample was taken for x-ray diffraction (XRD) and/or scanning electron microscope (SEM) analysis.

After roasting, the roasted EAF dust was leached with water at 95 to 97°C for 1 h, followed by filtration of the slurry, washing and drying of the solids, and collection of the filtrate and wash samples for analysis. A subsample of the solids was taken for XRD and SEM analysis and the remaining solids were then leached with 200 g/L H_2SO_4 for 1.5 h at room temperature, followed by filtration of the slurry, washing and drying of the solids, and collection of the filtrate and wash samples for analysis.

4.2. Design of Experiments (DOE) Tests

The effects of temperature, Na_2CO_3 addition, and secondary additions of either CaCO_3 or MnCO_3 on the zinc and iron extractions were further quantified through the use of a Design of Experiments (DOE) test. This test was conducted using a 2^3 circumscribed central composite design (CCD). A circumscribed central composite design consists of a standard 2^3 factorial design with the addition of center points to all

for quantification of nonlinearity in the response of output variables, and axial points to allow for the construction of response surface models (RSM) from the output variables. Input variables were selected for the axial points to produce a fully rotatable design (i.e., with the additional axial points of the design at a radius of $\alpha=(2^k)^{1/4}$ from the design centre) to allow RSM to be constructed from the output variables.

The conditions used for each sample in these DOE tests are shown in Table 2; samples were designated as matrix (M), centre (C) or axial (A) points, respectively, depending on their location relative to the centre of the design. Each individual sample for these tests was prepared using the roasting and leaching procedure outlined earlier.

Table 2 Input Variables for Each Sample Tested in the Design of Experiments Tests

Sample	Temperature, °C	Na ₂ CO ₃ Addition, %	Secondary Addition, %	
			CaCO ₃	MnCO ₃
M1	800	50.0	3.7	4.3
M2	800	50.0	14.1	16.3
M3	800	50.0	3.7	4.3
M4	800	90.0	14.1	16.3
M5	1000	50.0	3.7	4.3
M6	1000	50.0	14.1	16.3
M7	1000	90.0	3.7	4.3
M8	1000	90.0	14.1	16.3
C1	900	70.0	8.9	10.2
C2	900	70.0	8.9	10.2
A1	732	70.0	8.9	10.2
A2	1068	70.0	8.9	10.2
A3	900	36.4	8.9	10.2
A4	900	103.6	8.9	10.2
A5	900	70.0	0.17	0.19
A6	900	70.0	17.6	20.2

Lower additions of CaCO₃ (3.7 to 14.1%) and MnCO₃ (4.3 to 16.3%) were made than were used during the DOE tests using secondary additives for the La Oroya zinc ferrite [8]. These additions were determined based on the stoichiometric additions that would be required to form 100% MnFe₂O₄ or 100% CaFe₂O₄ (50% Ca₂Fe₂O₅) or from iron in the zinc ferrite component of the EAF dust.

A software package called DOE XL Pro (a trademark of Digital Computations, Inc. and Air Academy Associates, LLC) was used to assist in the experimental design, and aid in the analysis of the results and the construction of the response surface models from these results. The R² values for the response surface models for overall zinc and iron extractions were 0.898 and 0.945, respectively, for CaCO₃ and 0.884 and 0.986,

respectively for MnCO_3 . The R^2 value for the RSM for chromium extractions by water leaching was 0.765 for both CaCO_3 and MnCO_3 .

4.3. Chemical and Mineralogical Analysis

All solutions and solids were analyzed with atomic absorption spectroscopy (AA) with a single-element Perkin-Elmer 4000 instrument. Solids were digested by fusion with lithium metaborate at 950°C and dissolved in HCl prior to analysis.

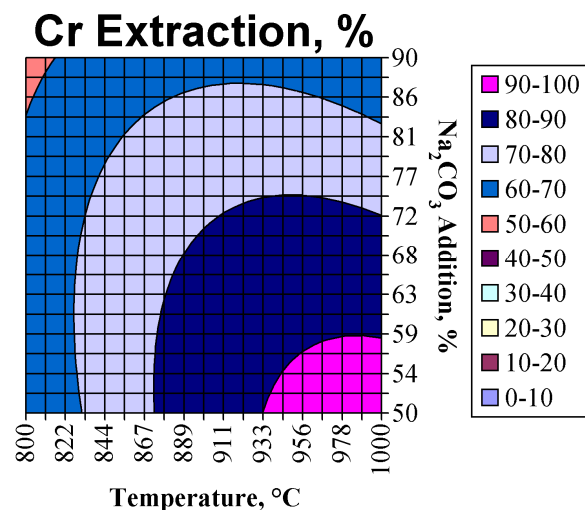
Scanning electron microscope analysis was performed on selected samples using a Hitachi Model S-2700 Microscope equipped with a GW Electronics Annular Four-Quadrant Backscattered Electron Detector and a Princeton Gamma Tech Prism Intrinsic Germanium (IG) x-ray detector and operating at an accelerating voltage of 20 kV. The digital images were taken using a Princeton Gamma Tech IMIX system.

X-ray diffraction analysis was performed using a Rigaku Rotoflex XRD with a rotating Cu anode. The x-ray patterns were then analyzed using Version 7 of the Jade software obtained from Materials Data, Inc.

5. RESULTS

The DOE tests for roasting Altasteel EAF dust with Na_2CO_3 reported in earlier work [7] were conducted at slightly lower temperatures and Na_2CO_3 additions than this study. Fig. 1 and Fig. 2 show an extrapolation of the RSM from this previous study to allow the results, and the effects of secondary additives, to be readily compared and quantified.

FIG 1. Extrapolation of the Response Surface Model Describing the Effect of Temperature and Na_2CO_3 Addition on the Extraction of Chromium from Roasted Altasteel EAF Dust by Leaching with Hot Water



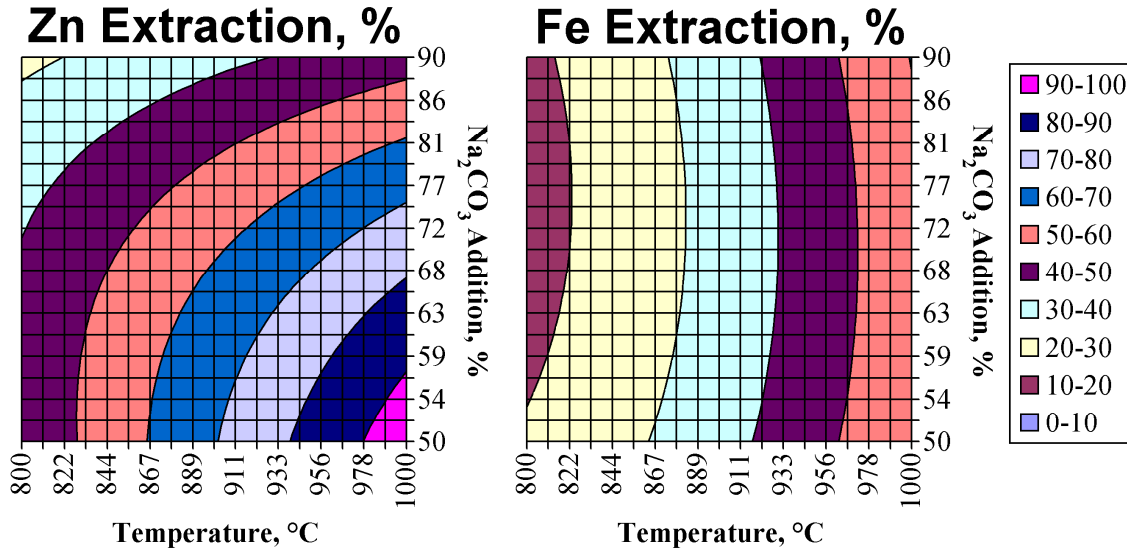


FIG 2. Extrapolation of the Response Surface Models Describing the Effect of Temperature and Na₂CO₃ Addition on the Extraction of Zinc and Iron from Roasted Altasteel EAF Dust after Leaching with 200 g/L H₂SO₄

5.1. Roasting with CaCO₃ as a Secondary Additive

5.1.1. Response Surface Models and Metals Extractions

The shape of the chromium and zinc extraction response surface models (Fig. 3 to Fig. 5) for leaching the roasted ash with water and 200 g/L H₂SO₄, respectively, closely follows the trends in extraction observed in the scoping tests and roasting with Na₂CO₃ alone (Fig. 1 and Fig. 2), with a maximum around 50% Na₂CO₃ and 1000°C and a decrease in extractions at higher Na₂CO₃ additions and lower temperatures. However, the addition of CaCO₃ as a secondary additive during roasting significantly broadened the area of maximum (90 to 100%) chromium extraction possible with water leaching (Fig. 3) and of the maximum zinc extraction possible with acid leaching (Fig. 4 and Fig. 5), even at low CaCO₃ additions. This makes extractions of over 90% possible over a wider range of temperatures and Na₂CO₃ additions. With increasing CaCO₃ additions, the region of maximum chromium extraction shrinks, while the region of maximum zinc extraction increases in size, making these extractions possible at lower temperatures and a broader range of Na₂CO₃ additions. Chromium extractions from water leaching, though, are consistently greater than 90% in the regions where zinc extractions are over 90%.

Iron extractions are greatly affected by the addition of CaCO₃ to the EAF dust during roasting. Iron extractions were 50 to 60% in the region where zinc extractions were over 90% for roasting with Na₂CO₃ alone (Fig. 2), but adding CaCO₃ during roasting causes iron extractions to increase to 60 to 90%, depending on the temperature, Na₂CO₃ and CaCO₃ addition used, for conditions where zinc extractions are greater than 90% (Fig. 4 and Fig. 5).

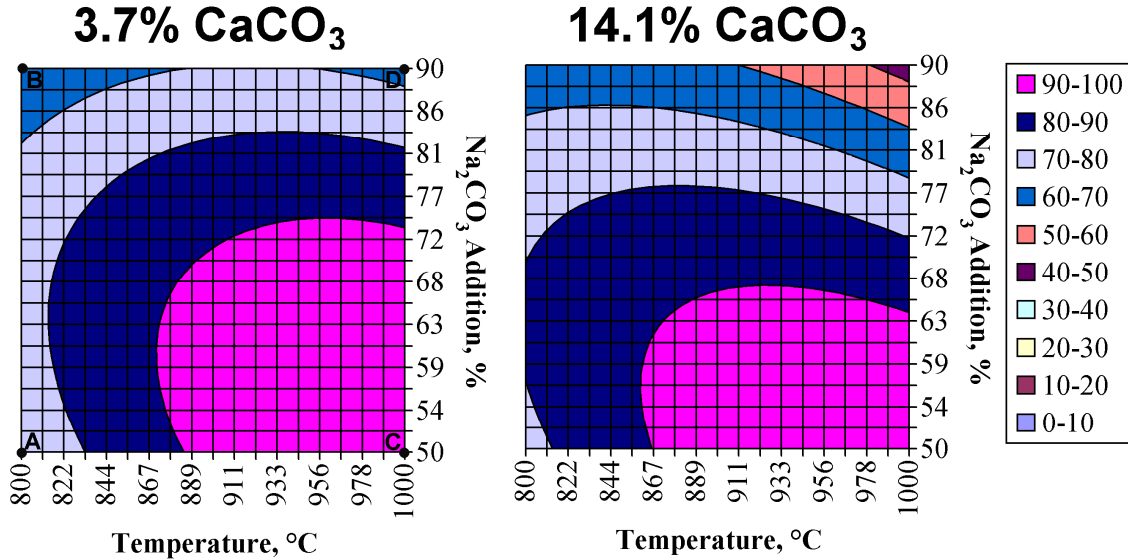


FIG 3. Effect of Na₂CO₃ and Temperature on Hot Water Leach Extractions of Chromium from Altasteel EAF Dust Roasted with CaCO₃

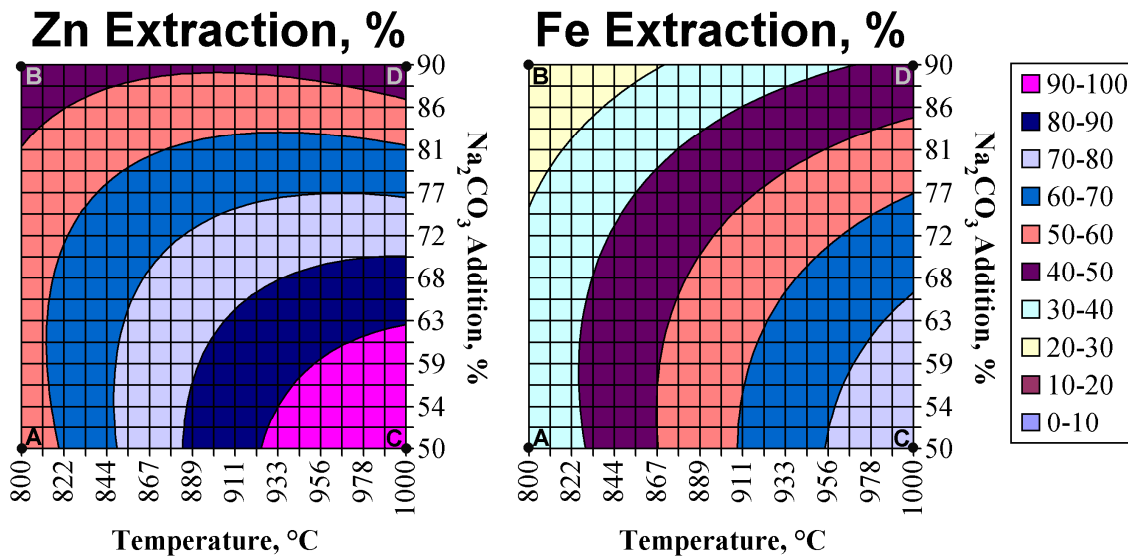


FIG 4. Effect of Na₂CO₃ and Temperature on Zinc and Iron Extractions from Altasteel EAF Dust Roasted with 3.7% CaCO₃ after Leaching with 200 g/L H₂SO₄

Furthermore, the iron extraction for roasting with CaCO₃ and Na₂CO₃ (Fig. 4 and Fig. 5) does not show the same trend as roasting with Na₂CO₃ alone (Fig. 2) where higher Na₂CO₃ additions cause an increase in iron extractions. Instead iron extractions increase with increasing temperature and decreasing Na₂CO₃ addition similar to the trend observed for zinc and chromium extractions.

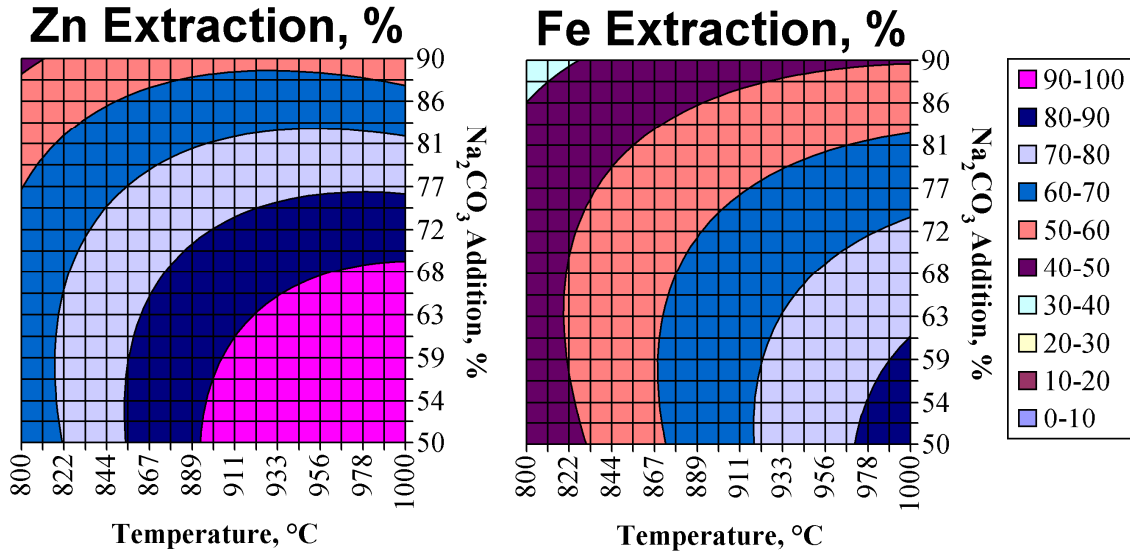


FIG 5. Effect of Na₂CO₃ and Temperature on Zinc and Iron Extractions from Altasteel EAF Dust Roasted with 14.1% CaCO₃ after Leaching with 200 g/L H₂SO₄

5.1.2. X-ray Diffraction Analysis

To try to correlate this behaviour to the phases formed during roasting, and remaining after leaching with 200 g/L H₂SO₄, samples at various conditions described by the model for roasting with Na₂CO₃ and the lowest CaCO₃ addition tested (3.7%) were analyzed using x-ray diffraction (Points A through D on Fig. 3 and Fig. 4). The diffraction patterns for the samples of EAF dust after roasting and after leaching are shown in Fig. 6 and Fig. 7, respectively, while the identified phases are listed in Tables 3 and 4, respectively.

Table 3 Phases Identified by XRD Analysis of EAF Dust Roasted with Na₂CO₃ and 3.7% CaCO₃

Sample	Identified Phases (in order of intensity)
A	α -NaFeO ₂ , Ca ₂ Fe ₂ O ₅ , (Zn,Mn,Fe)(Fe,Mn) ₂ O ₄ , ZnO
B	Ca ₂ Fe ₂ O ₅ , (Zn,Mn,Fe)(Fe,Mn) ₂ O ₄ , α -NaFeO ₂ , ZnO
C	α -NaFeO ₂ , Ca ₂ Fe ₂ O ₅ , ZnO, β -NaFeO ₂ , CaCO ₃
D	(Zn,Mn,Fe)(Fe,Mn) ₂ O ₄ , α -NaFeO ₂ , Ca ₂ Fe ₂ O ₅ , β -NaFeO ₂ , ZnO

Table 4 Phases Identified by X-ray Diffraction Analysis of EAF Dust after Roasting with Na₂CO₃ and CaCO₃ and Leaching with 200 g/L H₂SO₄

Sample	Identified Phases (in order of intensity)	Leaching Wt. Loss, %
A	(Zn,Mn,Fe)(Fe,Mn) ₂ O ₄ , CaSO ₄ ·2H ₂ O	24 ¹ , 67 ²
B	(Zn,Mn,Fe)(Fe,Mn) ₂ O ₄ , CaSO ₄ ·2H ₂ O	42 ¹ , 52 ¹
C	Ca ₂ Fe ₂ O ₅ , CaSO ₄ ·2H ₂ O	14 ¹ , 41 ²
D	(Zn,Mn,Fe)(Fe,Mn) ₂ O ₄ , CaSO ₄ ·2H ₂ O, Ca ₂ Fe ₂ O ₅	41 ¹ , 45 ²

¹ Hot Water Leach ² Acid Leach

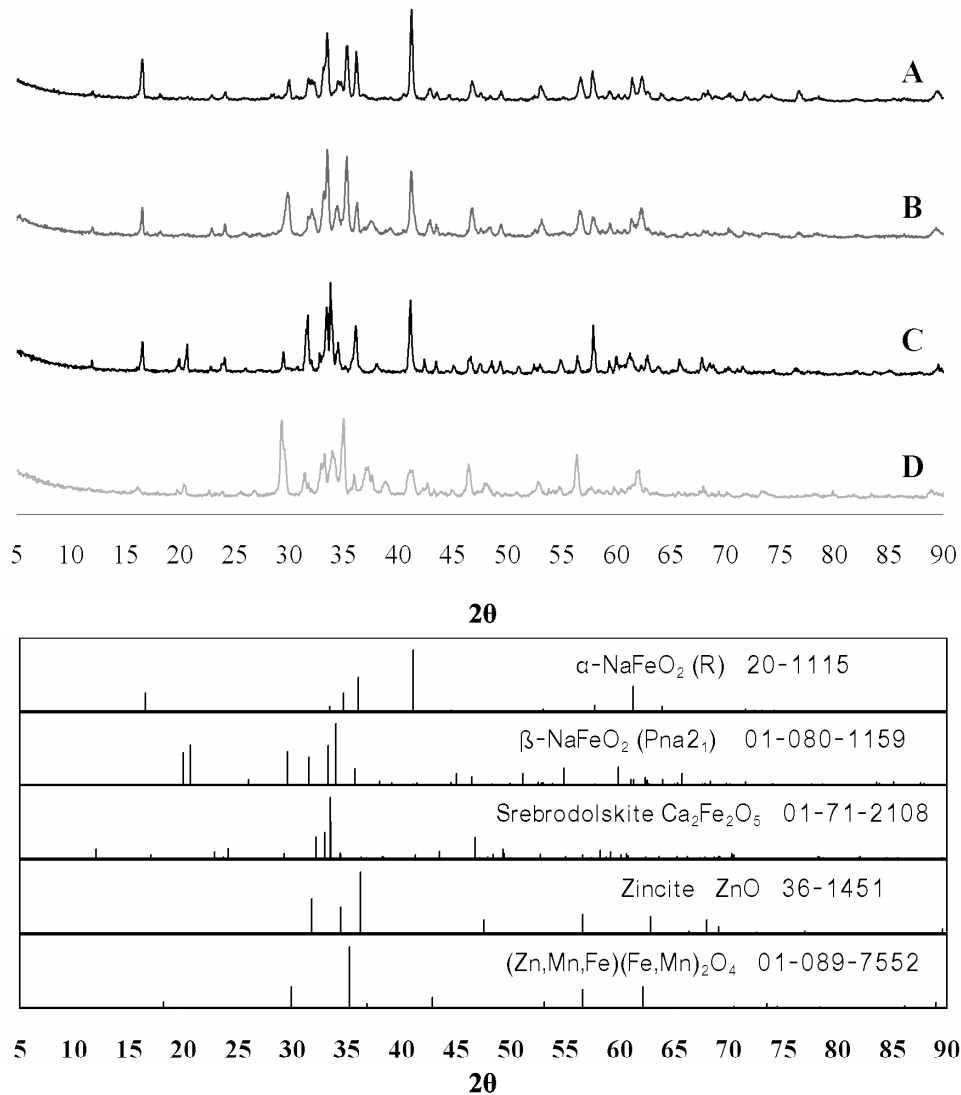


FIG. 6 XRD Patterns of EAF Dust Residue after Roasting with Na₂CO₃ and CaCO₃

Decomposition, or partial decomposition, of ZnFe₂O₄ occurs across the entire temperature range tested with NaFeO₂ and ZnO identified in all the samples tested after roasting using XRD. Srebrodolskite is also observed in all four samples, and is the major phase in Sample B, likely forming from the reaction of free calcium with magnetite (Fe₃O₄) or NaFeO₂. The absence of any residual Zn-Mn-Fe ferrite peaks in Sample C is consistent with the high zinc extractions observed for that sample, indicating that near complete decomposition of ZnFe₂O₄ occurs at these conditions. (Similarly, the lower zinc extractions in Sample D for higher Na₂CO₃ additions are consistent with the presence of (Zn,Mn,Fe)(Fe,Mn)₂O₄ in Sample D as the major phase.) Specific silicate phases could not be identified using x-ray diffraction but, based on the phases observed from roasting with Na₂CO₃ alone [7] and in the EAF dust feed, it is likely that the majority of silicon is

present in the roasted dust as larnite (Ca_2SiO_4). In these samples, the formation of α - NaFeO_2 is favored, even at higher temperatures, over β - NaFeO_2 ; this behaviour is consistent with the results from roasting this EAF dust with Na_2CO_3 alone [7], but differs from the results of roasting of the La Oroya zinc ferrite where β - NaFeO_2 is preferred at temperatures of 950°C and higher [10].

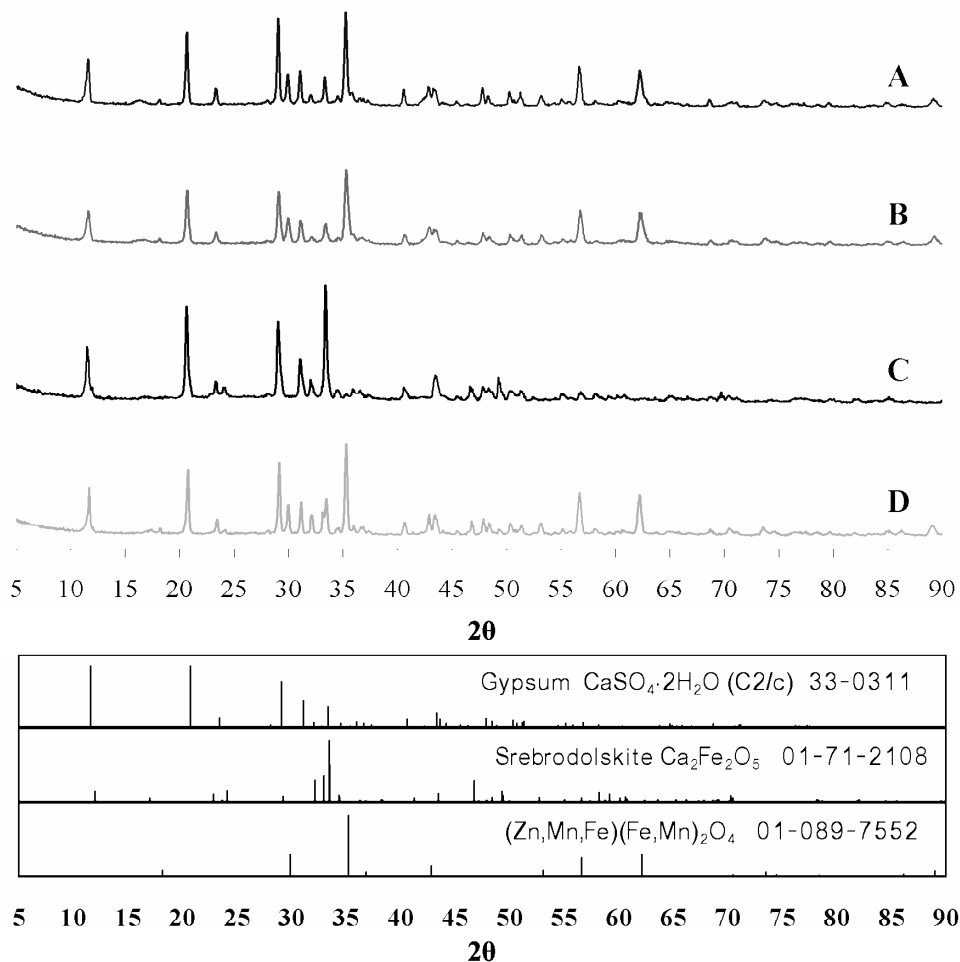


FIG. 7 XRD Patterns of EAF Dust Residue after Roasting with Na_2CO_3 and CaCO_3 and Leaching with 200 g/L H_2SO_4

After leaching with 200 g/L H_2SO_4 , gypsum ($\text{CaSO}_4 \cdot 2\text{H}_2\text{O}$) was identified in all the samples analyzed with x-ray diffraction (Table 4 and Fig. 7), with $(\text{Zn,Mn,Fe})(\text{Fe,Mn})_2\text{O}_4$ as the major phase in Samples A, B and D where zinc extractions were lower and absent from Sample C where high zinc extractions were observed. Srebrodolskite ($\text{Ca}_2\text{Fe}_2\text{O}_5$) is also detected in significant quantities in samples roasted at 1000°C (Samples C and D). (Even though srebrodolskite ($\text{Ca}_2\text{Fe}_2\text{O}_5$) was formed when roasting the EAF dust with Na_2CO_3 alone, it could not be detected by x-ray diffraction and could only be observed in trace quantities using SEM/EDX analysis after leaching with 200 g/L H_2SO_4 [7].)

5.1.3. Scanning Electron Microscopy/Energy Dispersive X-ray Analysis

Fig. 8 shows a micrograph of Sample C (1000°C, 50% Na₂CO₃, 3.7% CaCO₃) after roasting using back-scattered SEM imaging and EDX analysis. The zinc oxide (A) and srebrodolskite (C) phases identified using XRD are visible with the SEM, but a separate Na-Fe phase (i.e., NaFeO₂) was not detected in the field of view. Several other types of particles are observed, including particles high in Pb, Ca and O (i.e., PbO and CaO (B)), high in Ca, Mn, Fe and O (i.e., likely a mixture of MnFe₂O₄ and Ca₂Fe₂O₅ (D)), and high in Fe and O (i.e., Fe₃O₄ (E)), as well a darker phase containing Na, K and O (i.e., likely (Na,K)₂O (F)).

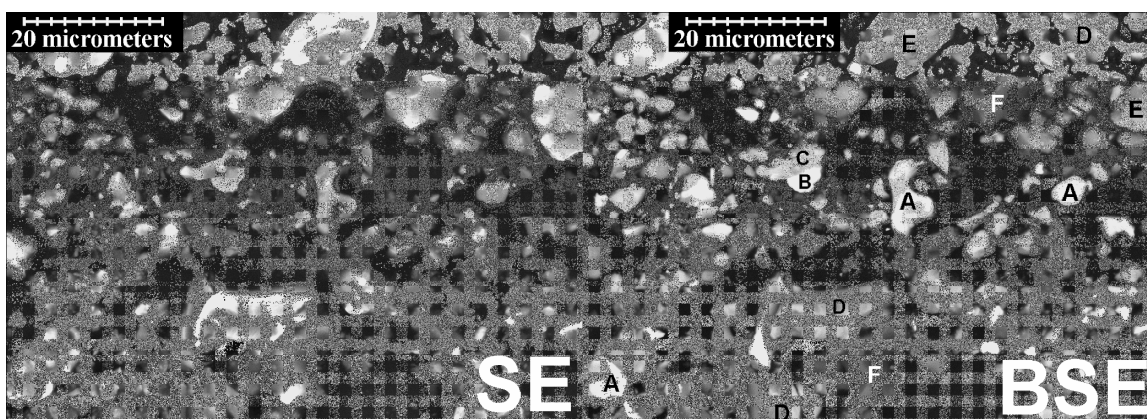


Fig. 8 Secondary Electron (SE) and Backscattered Electron (BSE) Images of EAF Dust after Roasting at 1000°C with 50% Na₂CO₃ and 3.7% CaCO₃ (Sample C)

After leaching with 200 g/L H₂SO₄, Samples C (1000°C, 50% Na₂CO₃, 3.7% CaCO₃) and D (1000°C, 90% Na₂CO₃, 3.7% CaCO₃) were reexamined using SEM/EDX analysis (Fig. 9 and Fig. 10) to try to better understand the iron deportment in this system. Gypsum (CaSO₄·2H₂O) is the major phase in the field of view in both samples and is labeled as phase G in both Fig. 9 and Fig. 10.

In Sample C (Fig. 9), several phases containing iron are identified, including particles high in Ca, Fe and O (i.e., Ca₂Fe₂O₅ (E)) and high in Fe, Mn, Zn and O (i.e., residual unreacted (Zn,Mn)Fe₂O₄ (D)). Several particles were also found to be high in Fe, Mn and O, but the ratio of manganese to iron in the EDX intensities differed, with some particles showing a ratio of intensities of Mn:Fe of between 2:1 and 3:1 (A, B) and others with a ratio of about 0.33:1 to 0.5:1 (C). Thus, this would indicate that some manganese may substitute for ferric iron in the Mn-ferrite structure, resulting in Mn-ferrites closer to the composition of Mn₂FeO₄ (particles A and B) while other Mn-ferrites are more typical of jacobsite (MnFe₂O₄) (particles C and F). (Particle B contains Ca, Pb and S, in addition to Mn, Fe and O, and is likely a mixture of Mn₂FeO₄, gypsum and anglesite (PbSO₄) while Particle F contains Ca, Mn, Fe and O and is likely a mixture of MnFe₂O₄ and Ca₂Fe₂O₅.)

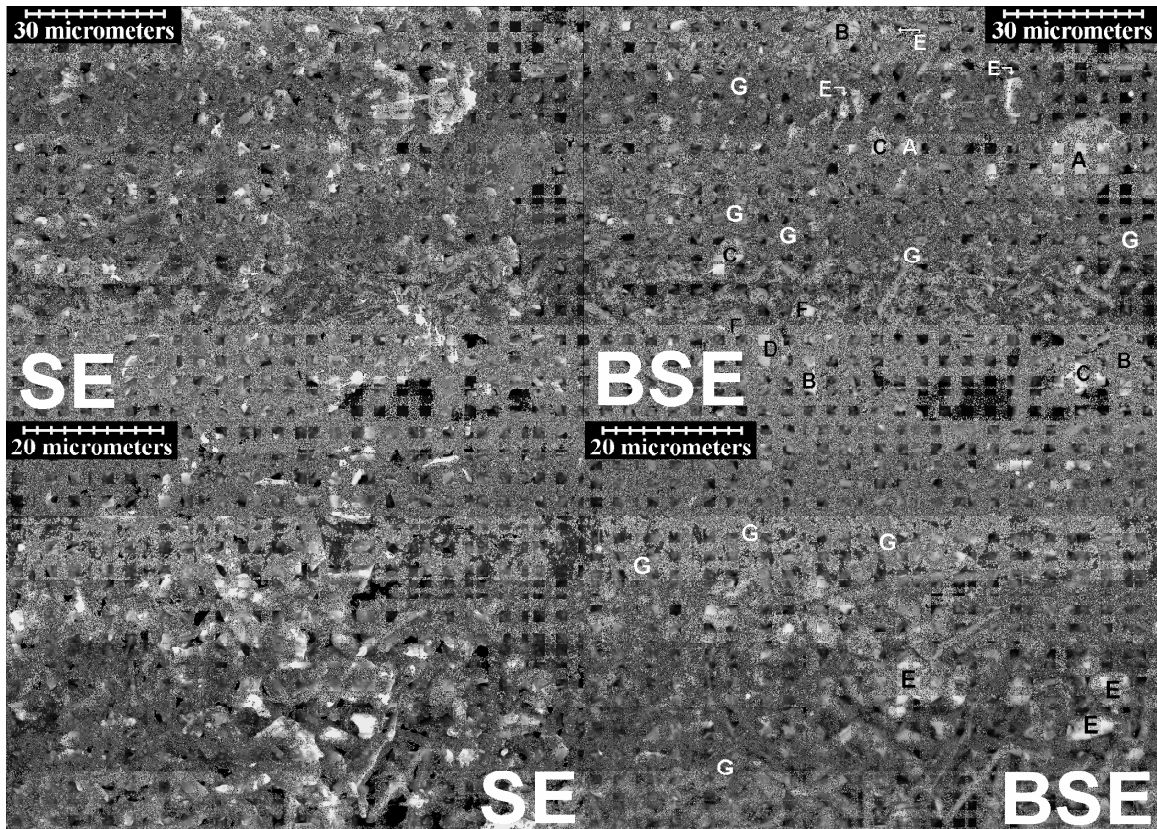


FIG. 9 Secondary Electron (SE) and Backscattered Electron (BSE) Images of EAF Dust after Roasting at 1000°C with 50% Na₂CO₃ and 3.7% CaCO₃ and Leaching with 200 g/L H₂SO₄ (Sample C)

In Sample D (Fig. 10), similar particles likely representing (Zn,Mn)Fe₂O₄ (A), MnFe₂O₄ (C), Ca₂Fe₂O₅ (D) and a mixture of Mn₂FeO₄ and gypsum (B) were identified. However, in Sample D, (Zn,Mn)Fe₂O₄ particles are much more abundant, due to the lower zinc extractions in this sample, and particles likely containing Mn₂FeO₄ are not observed as frequently as in Sample C.

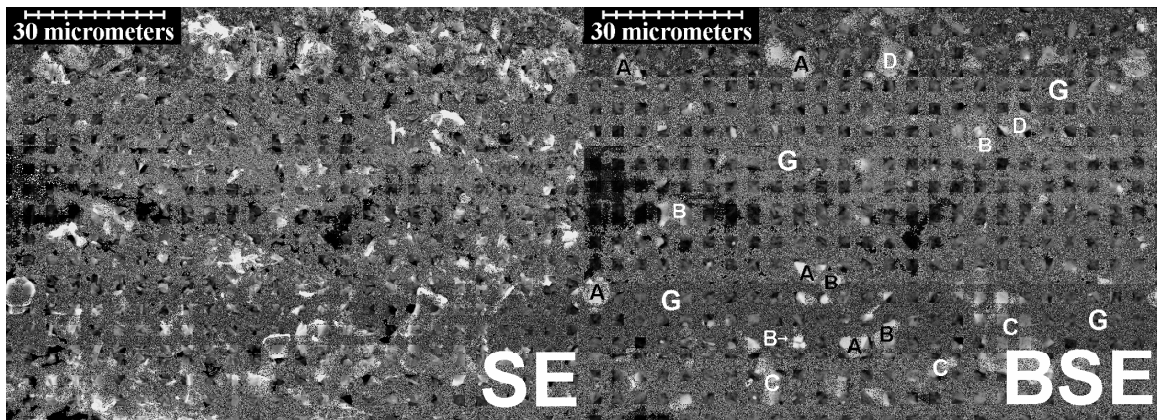


FIG. 10 Secondary Electron (SE) and Backscattered Electron (BSE) Images of EAF Dust after Roasting at 1000°C with 90% Na₂CO₃ and 3.7% CaCO₃ and Leaching with 200 g/L H₂SO₄ (Sample D)

5.1.4. Iron Department

The increase in iron extractions observed with the addition of CaCO_3 were not observed when roasting the La Oroya zinc ferrite with CaCO_3 , as a small, but steady decrease in iron extractions occurred with increasing CaCO_3 additions [8].

Thus, in order to explain this difference in behaviour, an iron balance for the roasting of EAF dust with Na_2CO_3 and CaCO_3 was then constructed using the chemical, x-ray diffraction and SEM/EDX analyses of the feed and of samples after roasting and after leaching (Table 5).

Table 5 Department of Iron Minerals during Roasting of EAF Dust with Na_2CO_3 and CaCO_3 and Leaching with 200 g/L H_2SO_4

Iron Minerals	% of Total Iron in Feed				
	Feed	Sample A	Sample B	Sample C	Sample D
ZnFe_2O_4	50.3	20.9	24.1	2.0	30.7
MnFe_2O_4	22.7	22.1	22.1	1.1 ^a	13.5 ^b
Mn_2FeO_4	0.0	0.0	0.0	5.3 ^a	2.3 ^b
Fe_3O_4	27.0	20.3	20.3	0.0	0.0
$\text{Ca}_2\text{Fe}_2\text{O}_5$	0.0	13.8	13.8	13.8	13.8
NaFeO_2	0.0	22.9	19.7	77.8	39.8
Total	100.0	100.0	100.0	100.0	100.0
Fe Extraction					
Projected, %		36.7 ¹	33.5 ¹	77.8 ²	39.8 ²
Actual, %		38.9	24.1	79.3	39.6
Difference, %		-2.2	9.4	-1.5	0.2

^a Calculated assuming 90% of Mn is present as Mn_2FeO_4

^b Calculated assuming 40% of the Mn is present as Mn_2FeO_4

¹ Calculated assuming the total dissolution of NaFeO_2 and $\text{Ca}_2\text{Fe}_2\text{O}_5$ during leaching

² Calculated assuming only the dissolution of NaFeO_2 during leaching

The iron balance for the feed is calculated assuming 100% of Zn and Mn in the feed are present as ZnFe_2O_4 and MnFe_2O_4 and the balance of the iron is present as Fe_3O_4 . The iron balance for Samples A to D is calculated, first, using zinc extractions to determine the conversion of ZnFe_2O_4 to NaFeO_2 and, second, assuming that Fe_3O_4 present in the dust after roasting is insoluble under the acid leaching conditions used. Third, it was assumed for this balance that the calcium in the feed that is not associated with silicon as Ca_2SiO_4 reacts with Fe_3O_4 to form $\text{Ca}_2\text{Fe}_2\text{O}_5$ while the CaCO_3 added during roasting reacted with NaFeO_2 to form $\text{Ca}_2\text{Fe}_2\text{O}_5$. (The assumption made in the iron balance for roasting with Na_2CO_3 alone that 100% of the available calcium reacts with magnetite to form $\text{Ca}_2\text{Fe}_2\text{O}_5$ [7] would lead to a significant overestimate of the iron extraction in Samples A and B.) Fourth, because srebrodolskite ($\text{Ca}_2\text{Fe}_2\text{O}_5$) is observed in the XRD and SEM/EDX analysis of the leach residue from Samples C and D, but not in Samples A and B, it was assumed that the $\text{Ca}_2\text{Fe}_2\text{O}_5$ formed at high temperatures was

insoluble (Samples C and D), but was still assumed to be leached completely at lower temperatures (Samples A and B). Fifth, it was assumed, based on the SEM/EDX analysis of Samples C and D, that some of the iron was present as Mn_2FeO_4 , instead of as MnFe_2O_4 , with the remaining iron assumed to react with Na_2CO_3 to form NaFeO_2 . (Without this assumption, complete leaching of $\text{Ca}_2\text{Fe}_2\text{O}_5$ and complete conversion of magnetite (Fe_3O_4) to NaFeO_2 in Sample C, with all the manganese as MnFe_2O_4 , would not explain the high iron extractions observed.) In Samples A and B, all the manganese was assumed to be present as MnFe_2O_4 .

With these assumptions, the balance agrees reasonably well with the iron extractions observed. However, the deportment of iron in samples roasted at 1000°C differs considerably from the iron deportment observed for roasting the Altasteel EAF dust with Na_2CO_3 alone [7] or roasting the La Oroya zinc ferrite with Na_2CO_3 [10] or with Na_2CO_3 and CaCO_3 [8].

Some of the phenomena can be readily explained. For example, the apparent decrease in the solubility of srebrodolskite ($\text{Ca}_2\text{Fe}_2\text{O}_5$) in H_2SO_4 solution former at higher roasting temperatures is consistent the results from tests performed by roasting the Altasteel EAF dust with coal and CaCO_3 which showed that, though srebrodolskite ($\text{Ca}_2\text{Fe}_2\text{O}_5$) is formed at all temperatures between 850 and 1050°C , the srebrodolskite formed at lower temperatures is leached more readily than that formed at higher temperatures. As well, the reaction of magnetite (Fe_3O_4) to form NaFeO_2 and $\text{Ca}_2\text{Fe}_2\text{O}_5$ has been proposed to explain the iron deportment during roasting of the EAF dust with Na_2CO_3 alone [7], although the extent of reaction increases significantly with the increase in temperature and Na_2CO_3 addition used in these tests.

However, some phenomena, such as the formation of $\text{Mn}(\text{Fe},\text{Mn})_2\text{O}_4$ spinels, are not as easily explained. Research on manganese iron spinels indicates that the formation of Mn_2FeO_4 is more likely where, instead of direct substitution of Mn^{3+} for Fe^{3+} in the octahedral sites, a combination of Mn^{4+} and Fe^{2+} are found in the octahedral sites, with Mn^{2+} remaining in the tetrahedral sites [11]. The results from roasting with Na_2CO_3 alone or roasting at lower temperatures with Na_2CO_3 and CaCO_3 would indicate that manganese is predominantly present as Mn^{2+} , leading to the formation of jacobsonite (MnFe_2O_4) spinels. Thus, if Mn^{2+} is the predominant manganese species, the formation of $\text{Mn}(\text{Fe},\text{Mn})_2\text{O}_4$ spinels would require the oxidation of manganese to Mn^{4+} . (Some ferrous iron should be present in the dust in the tetrahedral sites of magnetite (Fe_3O_4).) This is possible, considering that the roasting tests were conducted in air, but it is uncertain why this oxidation, and the formation of $\text{Mn}(\text{Fe},\text{Mn})_2\text{O}_4$ spinels, would be favored, or catalyzed, by the addition of even small amounts of CaCO_3 to the roasting system.

Nevertheless, these $\text{Mn}(\text{Fe},\text{Mn})_2\text{O}_4$ spinels do form, and based on the iron extractions in Fig. 5, their formation increases significantly with increasing CaCO_3 additions.

This type of behaviour, though, is not observed during Na_2CO_3 roasting of the La Oroya zinc ferrite at similar roasting temperatures and much higher CaCO_3 additions [8]. It is possible that this difference in behaviour may be related to the low crystallinity of the EAF dust, as outlined earlier and in other studies on this material [7]. If portions of the EAF dust are indeed poorly crystalline and, hence, metastable, then crystallization would be expected on heating and it is possible that, if crystallization occurs in the presence of other ionic compounds, such as CaCO_3 or CaO , more thermodynamically stable ferrites, such as $\text{Ca}_2\text{Fe}_2\text{O}_5$, may be formed preferentially. (The formation of calcium ferrites upon crystallization may reduce the amount of iron available to react with manganese in the dust to form MnFe_2O_4 type ferrites, thus, leading to the observed increase in the formation of Mn_2FeO_4 spinels.) Additional characterization and phase identification, though, would be required to be able to more confidently explain the mechanisms behind these observed phenomena and will be the subject of future research.

5.2. Roasting with MnCO_3 as a Secondary Additive

5.2.1. Response Surface Models and Metal Extractions

The shape of the chromium and zinc extraction response surface models (Fig. 11 to Fig. 14) for leaching the roasted ash with water and 200 g/L H_2SO_4 , respectively, closely follows the trends in extraction observed in the scoping tests for roasting with Na_2CO_3 (Fig. 1 and Fig. 2) or Na_2CO_3 - CaCO_3 (Fig. 3 to Fig. 5), with a maximum around 50% Na_2CO_3 and 1000°C and a decrease in extractions at higher Na_2CO_3 additions and lower temperatures. Increased MnCO_3 additions broaden the area of maximum (90 to 100%) chromium extraction possible with water leaching (Fig. 11), compared to roasting with Na_2CO_3 alone (Fig. 1), but the size of the area of the maximum zinc extractions (Fig. 12 to Fig. 14) is drastically decreased as MnCO_3 additions increase.

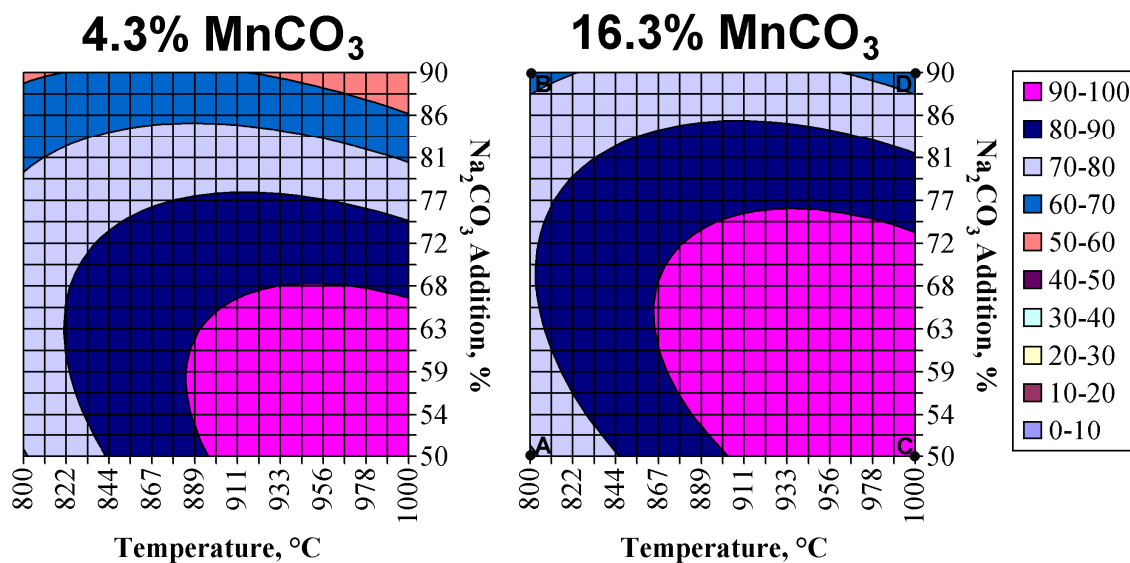


FIG. 11 Effect of Na_2CO_3 and Temperature on Chromium Extractions from Altasteel EAF Dust Roasted with MnCO_3

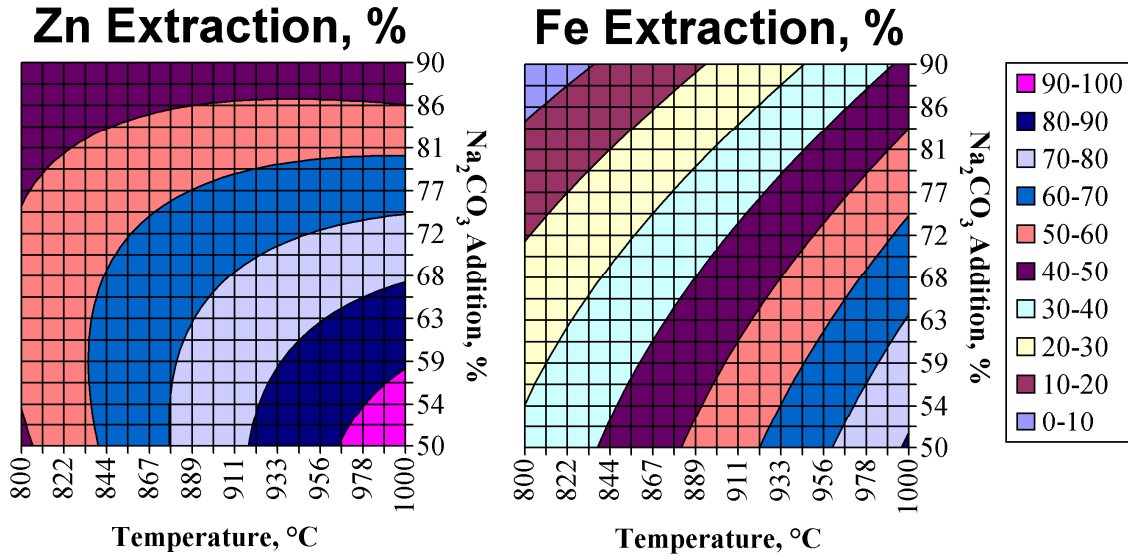


FIG. 12 Effect of Na₂CO₃ and Temperature on Zinc and Iron Extractions from Altasteel EAF Dust Roasted with 4.3% MnCO₃

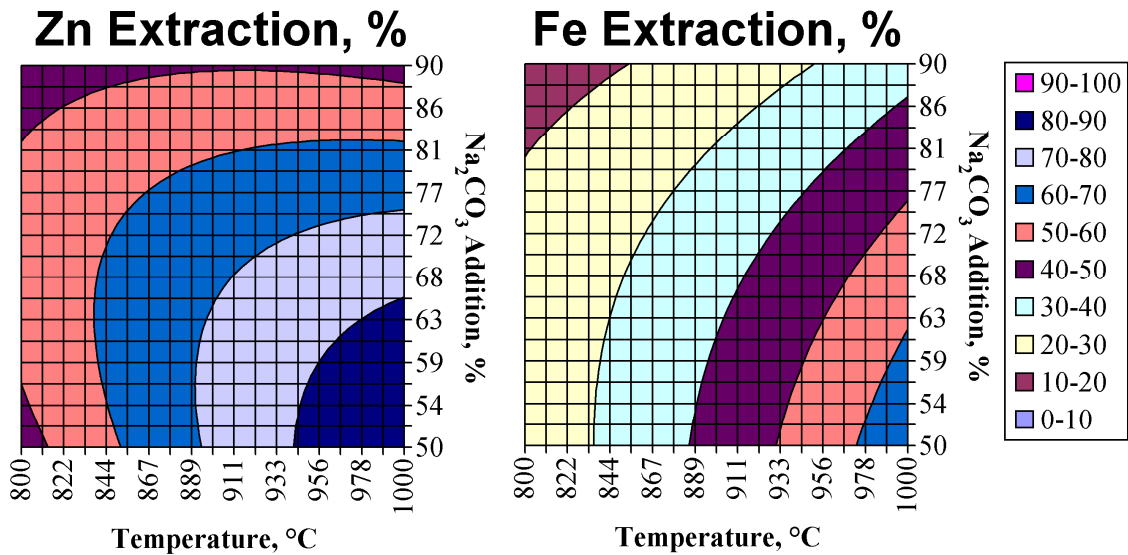


FIG. 13 Effect of Na₂CO₃ and Temperature on Zinc and Iron Extractions from Altasteel EAF Dust Roasted with 10.2% MnCO₃

Iron extractions are also affected by the addition of MnCO₃ to the EAF dust during roasting. While the overall iron extraction profile is similar in shape to that observed for roasting with Na₂CO₃ and CaCO₃ (Fig. 4 and Fig. 5), low MnCO₃ additions cause an initial increase in iron extractions to up to 80 to 90% in the region where zinc extractions were over 90% (Fig. 12) which is significantly higher than the 50 to 60% observed for roasting with Na₂CO₃ alone (Fig. 2). Additions of up to 16.3% MnCO₃ (Fig. 14) are required to return iron extractions to the levels observed when roasting with Na₂CO₃ alone (50 to 60%), but zinc extractions are drastically reduced at those MnCO₃ additions.

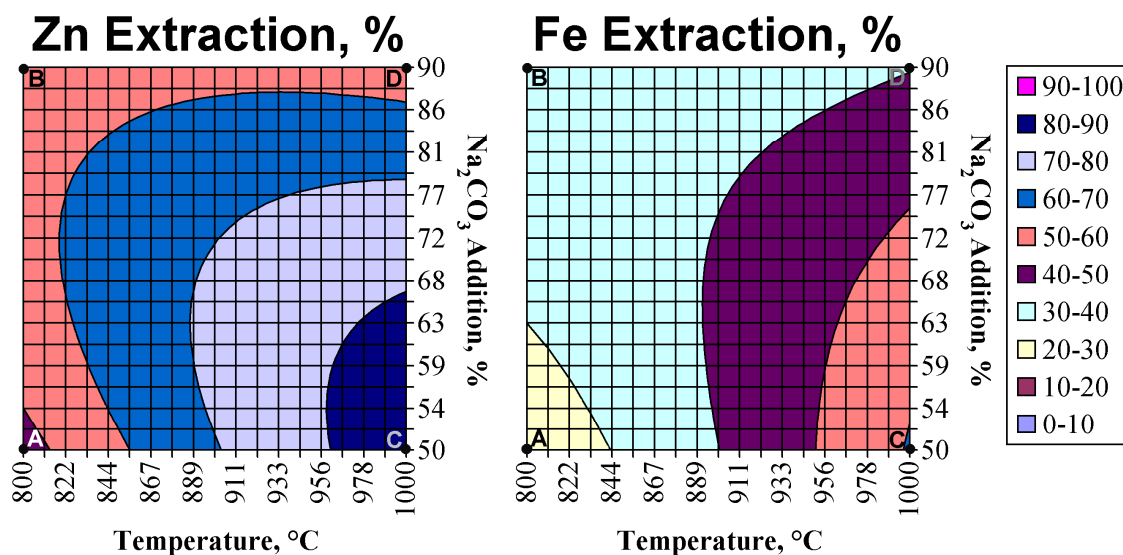


FIG. 14 Effect of Na₂CO₃ and Temperature on Zinc and Iron Extractions from Altasteel EAF Dust Roasted with 16.3% MnCO₃

5.2.2. X-ray Diffraction Analysis

Samples at various conditions described by the model for roasting with Na₂CO₃ and the highest MnCO₃ addition tested (16.3%) were analyzed using x-ray diffraction (Points A through D on Fig. 11 and Fig. 14) to try to correlate this behaviour to the phases formed during roasting, and remaining after leaching with 200 g/L H₂SO₄. The diffraction patterns for the samples of EAF dust after roasting and after leaching are shown in Fig. 15 and Fig. 16, respectively, while the identified phases are listed in Tables 6 and 7, respectively.

As with the x-ray diffraction analysis of La Oroya ferrite roasted with Na₂CO₃ and MnCO₃ [8], phase identification for the EAF dust samples roasted with MnCO₃ was less definitive than for EAF dust roasted with Na₂CO₃ or Na₂CO₃-CaCO₃. In several cases, x-ray diffraction peaks of significant intensity could not be positively identified from the available database. However, it was possible to positively identify several phases with x-ray diffraction including α -NaFeO₂, β -NaFeO₂, (Zn,Mn,Fe)(Fe,Mn)₂O₄, zincite (ZnO) and srebrodolskite (Ca₂Fe₂O₅), which are found in most of the samples tested. In Sample D, a calcium-manganese oxide (Ca₄Mn₃O₁₀) was also identified after roasting along with trace amounts of β -NaFeO₂.

After leaching with 200 g/L H₂SO₄, zincite (ZnO) and NaFeO₂ are dissolved, some calcium is dissolved and precipitated as gypsum (CaSO₄·2H₂O) and spinel phases, such as (Zn,Mn,Fe)(Fe,Mn)₂O₄, MnFe₂O₄ or Fe₃O₄, which were not dissolved during leaching were positively identified from x-ray diffraction on the leach residue (Table 7 and Fig. 16). However, several peaks could not be positively identified using the available database and software in these samples as well.

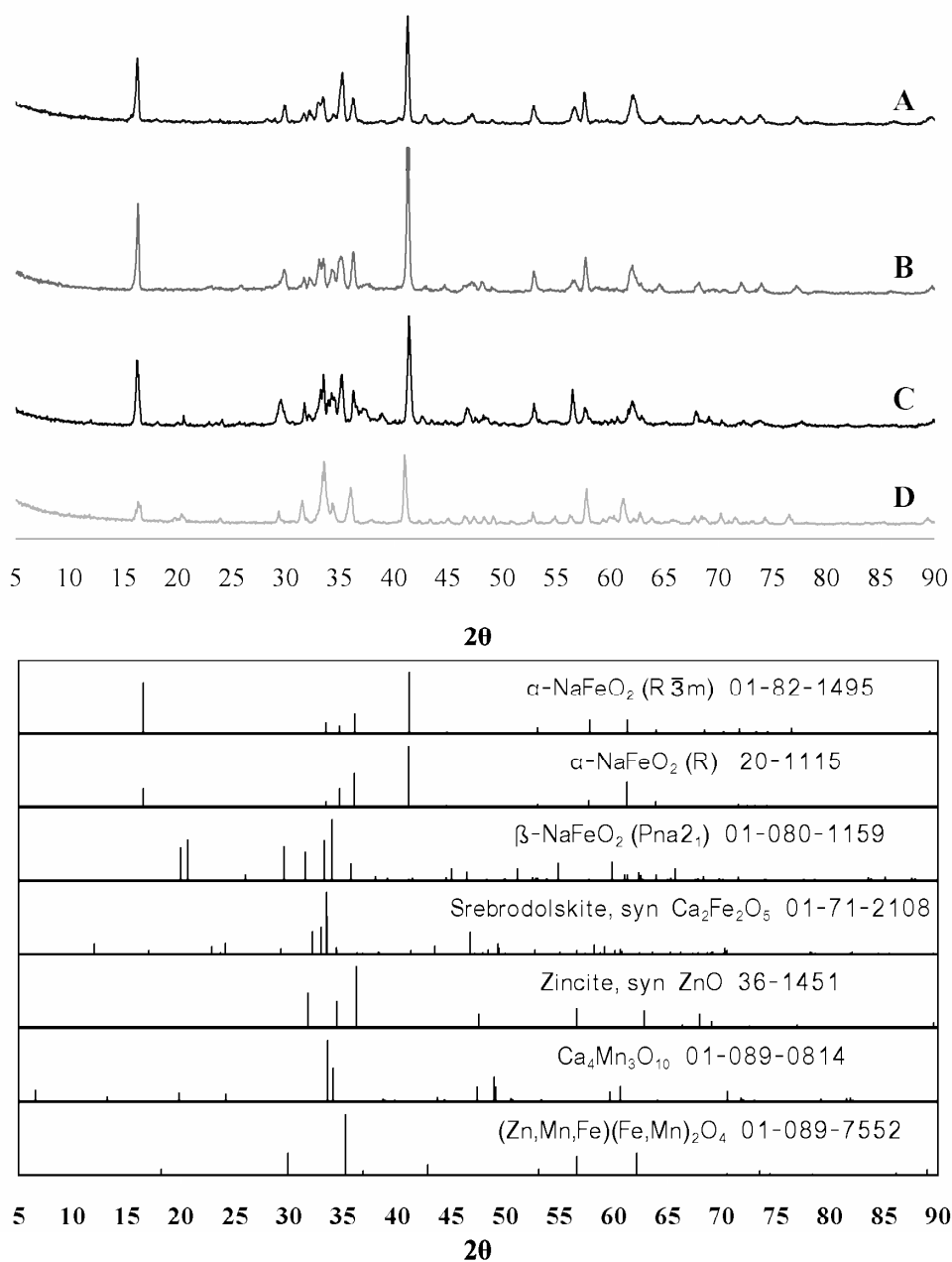


FIG. 15 XRD Patterns of EAF Dust Roasted with Na₂CO₃ and MnCO₃

Table 6 Phases Identified by XRD Analysis of EAF Dust Roasted with Na₂CO₃ and MnCO₃

Sample	Identified Phases (in order of intensity)
A	α -NaFeO ₂ , (Zn,Mn,Fe)(Fe,Mn) ₂ O ₄ , ZnO, Ca ₂ Fe ₂ O ₅
B	α -NaFeO ₂ , ZnO, (Zn,Mn,Fe)(Fe,Mn) ₂ O ₄ , ZnO, Ca ₂ Fe ₂ O ₅
C	α -NaFeO ₂ , Ca ₂ Fe ₂ O ₅ , (Zn,Mn,Fe)(Fe,Mn) ₂ O ₄ , ZnO
D	α -NaFeO ₂ , ZnO, Ca ₄ Mn ₃ O ₁₀ , Ca ₂ Fe ₂ O ₅ , β -NaFeO ₂

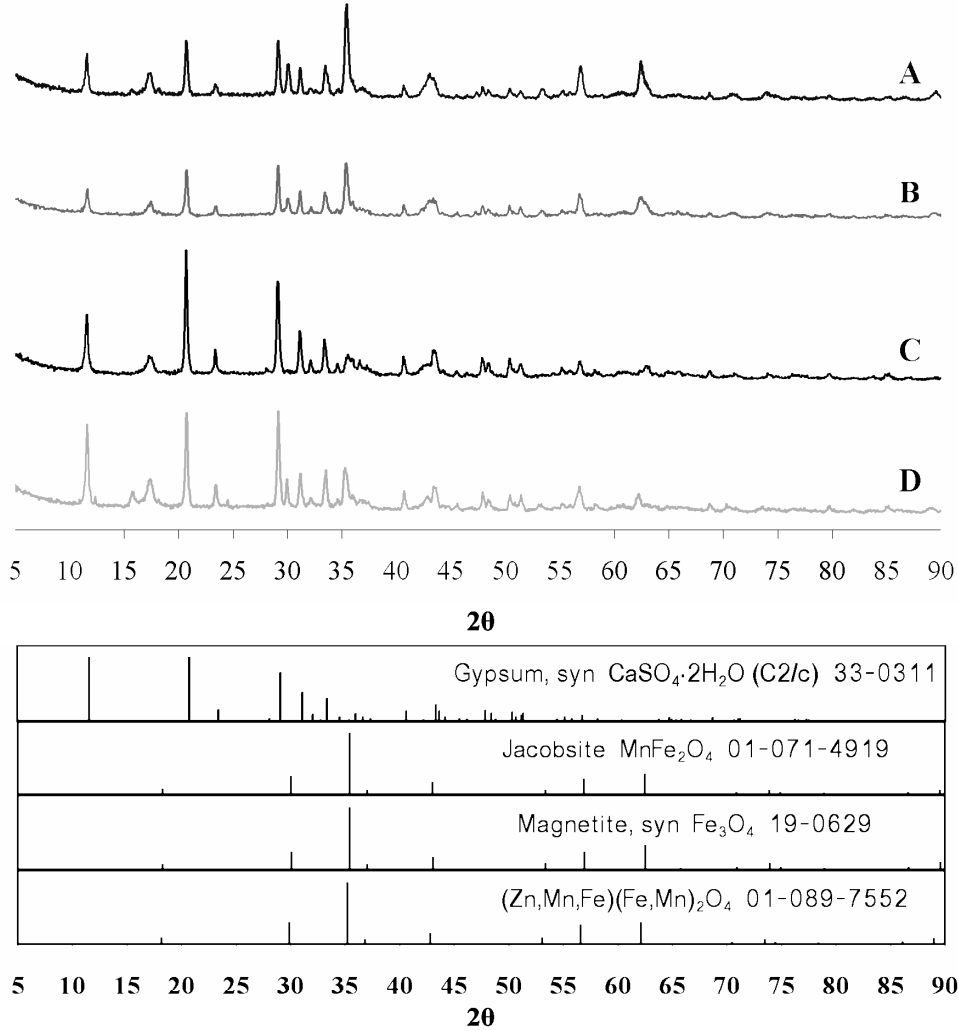


FIG. 16 XRD Patterns of EAF Dust Residue after Roasting with Na_2CO_3 and MnCO_3 and Leaching with 200 g/L H_2SO_4

Table 7 Phases Identified by X-ray Diffraction Analysis of EAF Dust after Roasting with Na_2CO_3 and MnCO_3 and Leaching with 200 g/L H_2SO_4

Sample	Identified Phases (in order of intensity)	Leaching Wt. Loss, %
A	$\text{CaSO}_4 \cdot 2\text{H}_2\text{O}$, $(\text{Zn}, \text{Mn}, \text{Fe})(\text{Fe}, \text{Mn})_2\text{O}_4$	19 ¹ , 72 ²
B	$\text{CaSO}_4 \cdot 2\text{H}_2\text{O}$, $(\text{Zn}, \text{Mn}, \text{Fe})(\text{Fe}, \text{Mn})_2\text{O}_4$	34 ¹ , 54 ²
C	$\text{CaSO}_4 \cdot 2\text{H}_2\text{O}$, $\text{MnFe}_2\text{O}_4/\text{Fe}_3\text{O}_4$	9 ¹ , 62 ²
D	$\text{CaSO}_4 \cdot 2\text{H}_2\text{O}$, $(\text{Zn}, \text{Mn}, \text{Fe})(\text{Fe}, \text{Mn})_2\text{O}_4$, $\text{MnFe}_2\text{O}_4/\text{Fe}_3\text{O}_4$	35 ¹ , 50 ²

¹ Hot Water Leach ² Acid Leach

5.2.3. Scanning Electron Microscopy/Energy Dispersive X-ray Analysis

Phase analysis using backscattered electron imaging in the scanning electron microscope and EDX analysis was performed on Sample C (1000°C, 50% Na₂CO₃, 16.3% MnCO₃), where the highest zinc extractions for this MnCO₃ addition were observed (Fig. 17 and Fig. 18). This analysis provided a much clearer picture of the phases present in the roasted EAF dust than x-ray diffraction.

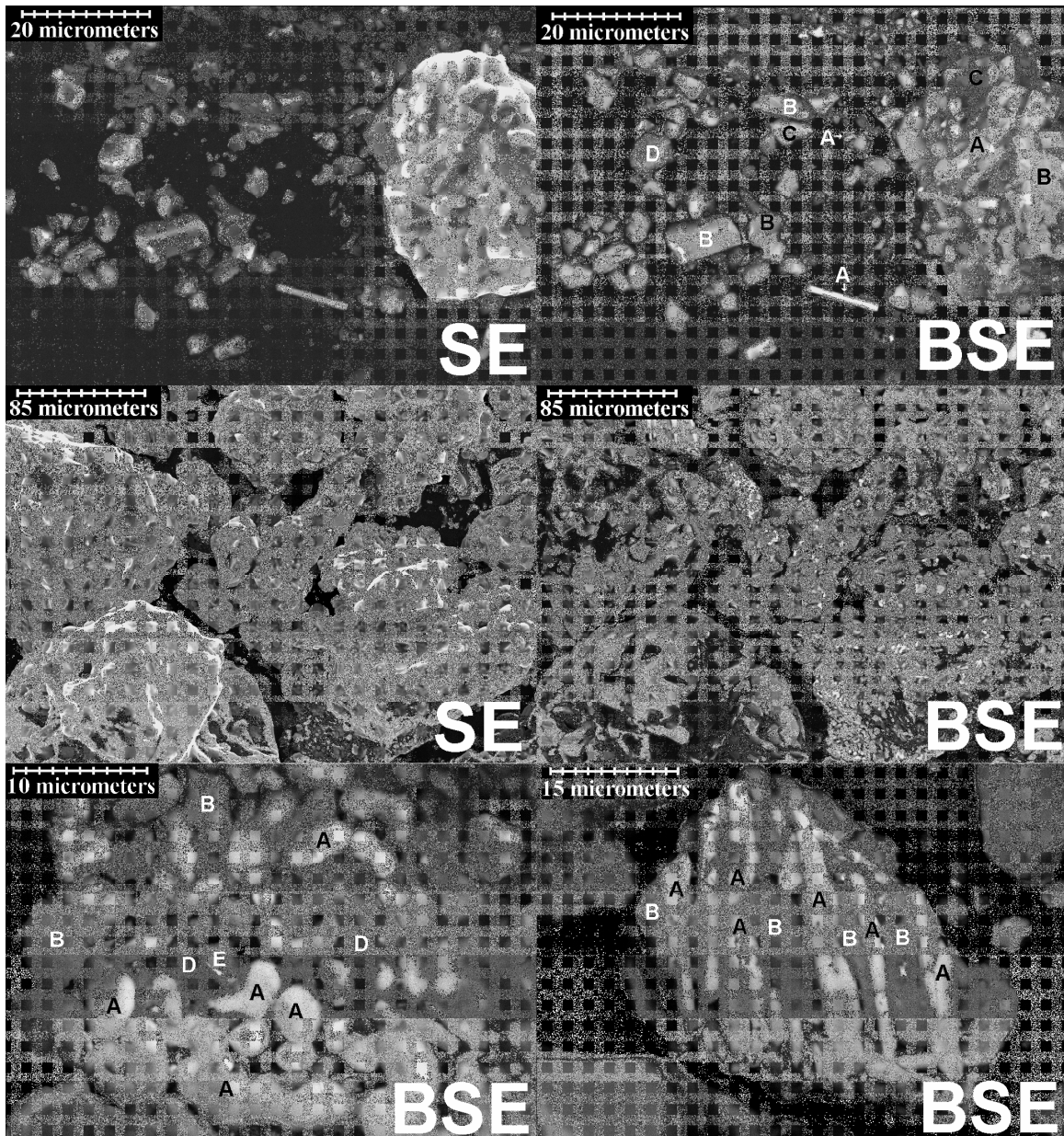


FIG. 17 Secondary Electron (SE) and Backscattered Electron (BSE) Images of EAF Dust after Roasting at 1000°C with 50% Na₂CO₃ and 16.3% MnCO₃ (Sample C)

After roasting, zinc oxide is visible as bright particles (A) in the backscattered images in Sample C (Fig. 17). Ferrites containing Mn, Fe and O (i.e., MnFe_2O_4 (B)) are the dominant iron bearing phase identified, but particles high in Ca, Fe and O (i.e., CaFe_2O_5 (C)) are also identified and both are consistent with the phases detected using x-ray diffraction. In addition, some darker particles were shown to be high in Ca, Si and O (i.e., Ca_2SiO_4 (D)) or high in Ca and O (i.e., $\text{CaO}/\text{Ca}(\text{OH})_2$ (E)). The particles in view in some of the SEM micrographs are very interesting texturally, showing what appear to be lamellar type layers of MnFe_2O_4 and ZnO in some particles.

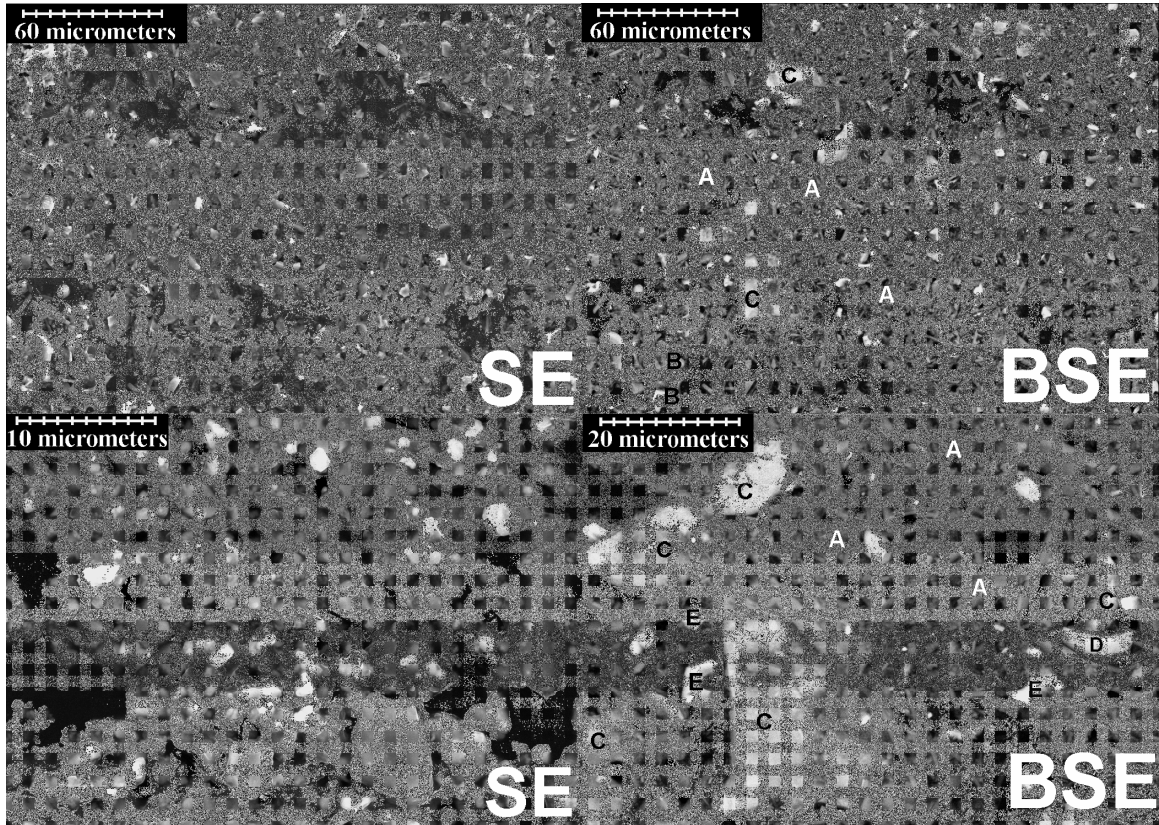


FIG. 18 Secondary Electron (SE) and Backscattered Electron (BSE) Images of EAF Dust after Roasting at 1000°C with 50% Na_2CO_3 and 16.3% MnCO_3 and Leaching with 200 g/L H_2SO_4 (Sample C)

After leaching with 200 g/L H_2SO_4 , the leach residue for Sample C showed gypsum (A), present as fine elongate crystals, as the major phase and likely forms because of the dissolution of larnite (Ca_2SiO_4) and reprecipitation of the dissolved calcium as gypsum during leaching (Fig. 18). Iron is present mostly as metal ferrites, with particles high in Fe, Mn and O (i.e., MnFe_2O_4 (B)) or high in Fe, Mn, Zn and O (i.e., $(\text{Zn,Mn})\text{Fe}_2\text{O}_4$ (C)) being the most common in the SEM micrograph and particles high in Ca, Fe and O (i.e., $\text{Ca}_2\text{Fe}_2\text{O}_5$ (E)) present in smaller quantities. (The presence of significant amounts of $(\text{Zn,Mn})\text{Fe}_2\text{O}_4$ would be expected, with zinc extractions of less than 90% at these roasting conditions.) Iron is also found in Particle D, which contains Fe, Mn, Si and O, likely as a Mn-Fe silicate.

5.2.5. Iron and Zinc Department

From the above analysis, it is evident that the addition of MnCO_3 promotes the formation of acid insoluble Mn-ferrites during roasting. This is indicated, first of all, by the detection of Mn ferrites using SEM/EDX analysis both before and after leaching and, second, by the decrease in iron extractions observed with increased MnCO_3 additions during roasting. However, for roasting this sample of EAF dust with Na_2CO_3 and MnCO_3 , several phenomena remain unexplained.

First, small additions of MnCO_3 (4.3%) cause an initial increase in the iron extractions observed, compared to those from roasting with Na_2CO_3 alone, and additions of up to 16.3% are required to return iron extractions to those observed from roasting with Na_2CO_3 alone. (In contrast, iron extractions from roasting La Oroya zinc ferrite with MnCO_3 cause a steady decrease in iron extractions, compared to roasting with Na_2CO_3 alone.) In roasting with low CaCO_3 additions, as discussed earlier, significant amounts of Mn_2FeO_4 , or other manganese rich ferrites, formed, resulting in less iron associated with manganese and, thus, more iron available to react with Na_2CO_3 to form acid soluble iron compounds. A similar phenomenon may occur during roasting of the EAF dust with MnCO_3 , resulting, initially, in higher iron extractions and, then, in a steady decrease in iron extractions with higher MnCO_3 additions as MnCO_3 reacts with NaFeO_2 to form MnFe_2O_4 .

Second, increased MnCO_3 additions drastically decrease the zinc extractions possible at a given temperature. A similar phenomenon is observed for roasting La Oroya zinc ferrite with MnCO_3 , but the effect is much less significant, even at MnCO_3 additions of up to 35% [8]. The behaviour could be caused either by the presence of a ZnFe_2O_4 - MnFe_2O_4 solid solution in the EAF dust initially, or by its formation during roasting, either by crystallization of the EAF dust after heating in the presence of Mn either in the dust or added as MnCO_3 , or by reaction of ZnFe_2O_4 in the EAF dust with the manganese added as MnCO_3 . (Tests indicate that, at high temperatures, MnCO_3 added without the addition of Na_2CO_3 to La Oroya zinc ferrite readily reacts to form a ZnFe_2O_4 - MnFe_2O_4 solid solution leading to a low zinc extraction [8,12].) If the majority of the zinc is present as a solid solution in $(\text{Zn,Mn})\text{Fe}_2\text{O}_4$, then it is possible that the increase in manganese content could decrease the activity of ZnFe_2O_4 in the roasting reactions, which, in turn, could decrease the zinc extractions possible after roasting.

To examine this possibility, calculations were made to determine the effect of ZnFe_2O_4 activity on the thermodynamics of the roasting reaction ($\text{ZnFe}_2\text{O}_4 + \text{Na}_2\text{CO}_3 \rightarrow 2 \text{NaFeO}_2 + \text{ZnO} + \text{CO}_2$ ($\Delta G^\circ = 163 - 0.149T$ (kJ/mol))) using the equation, $\Delta G = \Delta G^\circ + RT \ln K$. Several assumptions were made in these calculations, including assuming that all the manganese in the feed, and that added as MnCO_3 during roasting, reacts to form a solid solution of $(\text{Zn,Mn})\text{Fe}_2\text{O}_4$, that the activity of ZnFe_2O_4 in that solid solution is defined by Raoult's law (i.e., ideal solution), that P_{CO_2} is approximately 1 atm close to the reaction surface, that little change occurs in the activities of the other solids in the equilibrium constant expression over the temperature range considered (i.e., $a_{\text{solids}} \approx 1$, and, thus, $K \approx 1/a_{\text{ZnFe}_2\text{O}_4}$) and that the maximum zinc extraction occurs where

the activity of ZnFe_2O_4 is lowered enough to cause ΔG to equal zero for a given temperature. Based on these assumptions, Fig. 19 was constructed to compare the theoretical maximum extractions from these activity and thermodynamic calculations with the extractions observed for roasting with 50% Na_2CO_3 for each temperature from the response surface models (Fig. 12 to Fig. 14) for each level of MnCO_3 used in the DOE tests.

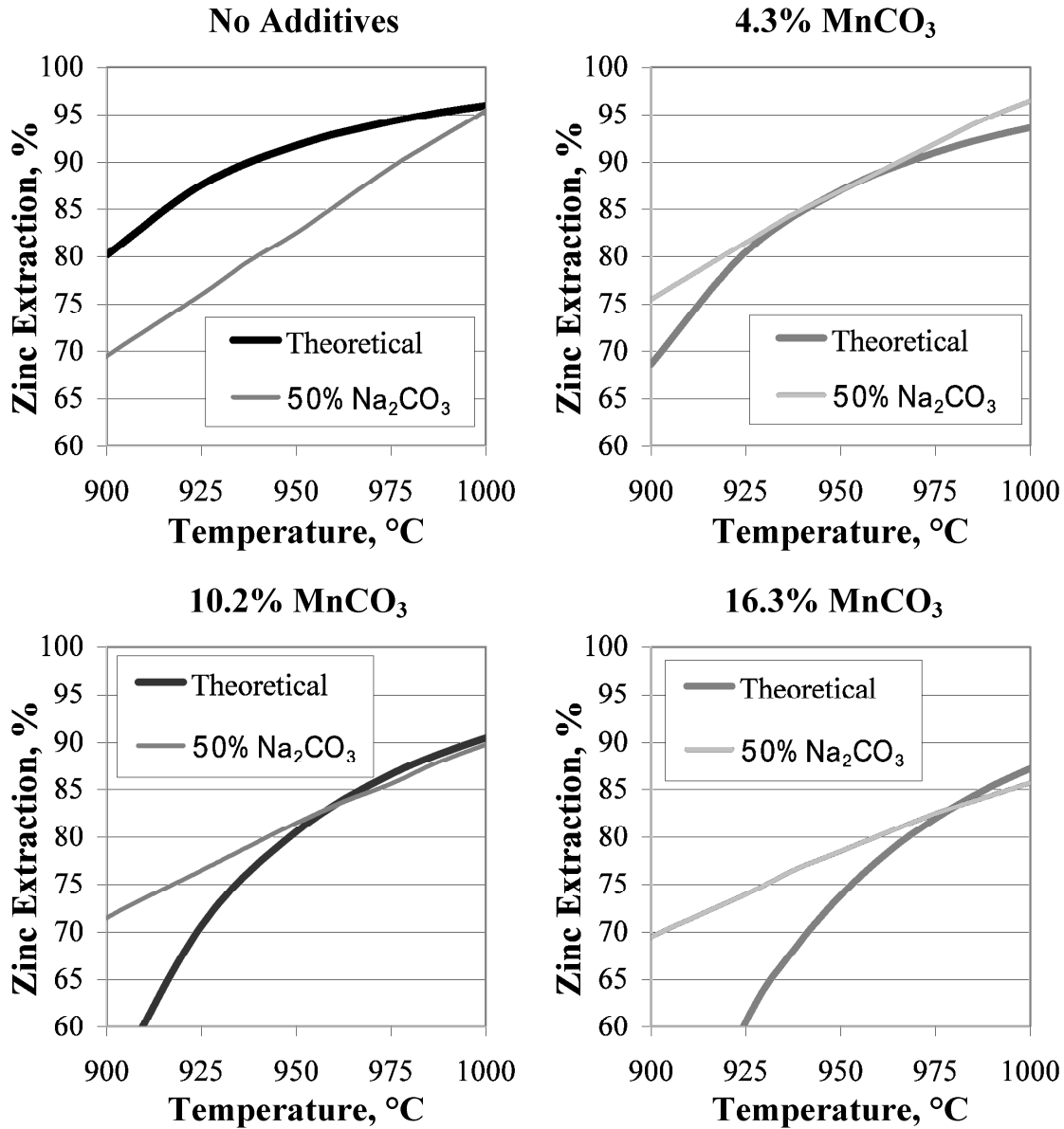


FIG. 19 Comparison of Maximum Zinc Extractions and Zinc Extractions at 50% Na_2CO_3 , from the Response Surface Models (RSM) with Maximum Extractions Calculated from the Change in Activity in a $(\text{Zn},\text{Mn})\text{Fe}_2\text{O}_4$ Solid Solution

Fig. 19 clearly shows a decrease in the theoretical zinc extraction with an increase in the MnCO_3 addition, which is a trend that is consistent with the experimental results, as is the observed trend of increasing maximum zinc extraction with increasing roasting temperature. Without MnCO_3 added, the theoretical and experimental zinc extractions do not agree closely, except at 1000°C , and the curves diverge above that temperature. With 4.3% MnCO_3 , the curves agree between 925 and 975°C but diverge at lower or higher temperatures. However, as the MnCO_3 additions are increased further, the discrepancy between the maximum theoretical and experimental zinc extractions decrease to the point that the curves converge above 950°C for 10.2% MnCO_3 addition and above 975°C for 16.3% MnCO_3 . Thus, it is probable that, at higher roasting temperatures, as MnCO_3 additions are increased, the activity of ZnFe_2O_4 in the $(\text{Zn},\text{Mn})\text{Fe}_2\text{O}_4$ spinel solid solution does affect the maximum zinc extractions possible during roasting of this sample of EAF dust with Na_2CO_3 . Thus, this behaviour would be expected to make it increasingly difficult to obtain high zinc extractions with high MnCO_3 additions.

6. CONCLUSIONS

From these results, neither CaCO_3 nor MnCO_3 was effective as a secondary additive to reduce iron extractions during roasting with Na_2CO_3 . Roasting with CaCO_3 increases the amount of iron dissolved in acid leaching. Iron extractions also increase initially with the addition of MnCO_3 , but decrease with increasing MnCO_3 additions; however, zinc extractions decreased significantly with increasing MnCO_3 additions and no improvement in iron extractions over roasting with Na_2CO_3 alone was observed.

From the mineralogical analysis, these process outcomes occur because the addition of secondary additives to the Altasteel EAF dust caused significant changes mineralogically compared to roasting with Na_2CO_3 alone. Even low CaCO_3 additions were shown to promote the formation of manganese rich iron oxides (e.g., Mn_2FeO_4) which reduced the amount of iron associated with acid insoluble Mn-ferrites and caused more iron to react with Na_2CO_3 to form acid soluble NaFeO_2 during roasting. Low additions of MnCO_3 may have had a similar effect, but larger MnCO_3 additions appear to have encouraged the formation of a ZnFe_2O_4 - MnFe_2O_4 solid solution while roasting at temperatures above 950°C which led to lower overall zinc recoveries during acid leaching.

Because of the significant differences observed after comparison with roasting a more crystalline material (i.e., the La Oroya zinc ferrite) with similar secondary additives, it is likely that this reaction behaviour may be related to the low crystallinity of the Altasteel EAF dust as, at the high roasting temperatures tested, the ionic compounds added as secondary additives may produce changes in the initial mineralogy of the EAF dust as it crystallizes upon heating which can significantly affect the results observed from roasting with Na_2CO_3 .

ACKNOWLEDGEMENTS

The authors would like to thank Altasteel, a division of Scaw Metals Group, for supplying a sample of electric arc furnace dust for metallurgical testing. The authors would also like to thank NSERC and Alberta Ingenuity for supplying student funding that helped support this research.

REFERENCES

- [1] Li, C. L. and Tsai, M. S., 1993, "Mechanism of spinel ferrite dust formation in electric arc furnace steelmaking." *ISIJ Int.*, Vol. 33, No. 2, pp.284-90.
- [2] Xia, D. K. and Pickles, C. A., 1998, "Extraction of nonferrous metals from electric arc furnace dust", In: *Waste Processing and Recycling in Mineral and Metallurgical Industries III*, pp.221-245, (Rao, S. R., Ed.) Montreal, QC Canadian Institute of Mining, Metallurgy and Petroleum.
- [3] Liebman, M., 2000, "The current status of electric arc furnace dust recycling in North America", *International Symposium on Recycling of Metals and Engineered Materials, 4th*, pp.237-250, (Stewart, D. L. Jr., Daley, J. C. and Stephens, R. L. Eds.), Warrendale, Pa, Minerals, Metals & Materials Society.
- [4] Zunkel, A. D., 2000, "Recovering zinc and lead from electric arc furnace dust: a technology status report", *International Symposium on Recycling of Metals and Engineered Materials, 4th*, pp.227-236, (Stewart, D. L. Jr., Daley, J. C. and Stephens, R. L. Eds.), Warrendale, Pa, Minerals, Metals & Materials Society.
- [5] Zunkel, A. D., 1997, "Electric arc furnace dust management: a review of technologies", *Iron and Steel Eng.*, Vol. 74, No. 3, pp.33-38.
- [6] Mager, K., Meurer, U., Garcia-Egocheaga, B., Goicoechea, N., Rutten, J., Saage, W., and Simonetti, F., 2000, "Recovery of zinc oxide from secondary raw materials: new developments of the Waelz process", *International Symposium on Recycling of Metals and Engineered Materials, 4th*, pp.329-344, (Stewart, D. L. Jr., Daley, J. C. and Stephens, R. L. Eds.), Warrendale, Pa, Minerals, Metals & Materials Society.
- [7] Holloway, P.C. and Etsell, T.H., "Roasting of Altasteel Electric Arc Furnace Dust with Na_2CO_3 ," submitted to *Metall. Trans. B*.
- [8] Holloway, P.C. and Etsell, T.H., "The Use of Secondary Additives to Control the Iron Dissolution during Na_2CO_3 Roasting of La Oroya Zinc Ferrite," submitted to *Metall. Trans. B*.
- [9] Johannsen, R., 2006, Private communication, Altasteel, Edmonton, AB, Canada.
- [10] Holloway, P.C. and Etsell, T.H., "Roasting of La Oroya Ferrite with Na_2CO_3 ", submitted to *Metall. Trans. B*.
- [11] Eschenfelder, A. H., 1958, "Ionic valences in manganese-iron spinels", *J. Appl. Phys.*, Vol. 29, pp.378-80.
- [12] Holloway, P.C., 2006, "Application of Transformational Roasting to the Treatment of Metallurgical Wastes," *Ph.D. Thesis, University of Alberta*.